Bioconjugate Chemistry

Article

pubs.acs.org/bc

The Complex Fate in Plasma of Gadolinium Incorporated into High-Density Lipoproteins Used for Magnetic Imaging of Atherosclerotic Plaques

Alessandra Barazza,[†,‡] Courtney Blachford,[†] Orli Even-Or,[†] Victor A. Joaquin,[†] Karen C. Briley-Saebo,[‡] Wei Chen,[‡] Xian-Cheng Jiang,[§] Willem J. M. Mulder,[‡] David P. Cormode,[‡] Zahi A. Fayad,[‡] and Edward A. Fisher*[,†]

[†]Leon H. Charney Division of Cardiology and Marc and Ruti Bell Program in Vascular Biology, Department of Medicine, New York University School of Medicine, Smilow 7, 522 First Avenue, New York, New York 10016, United States

[‡]Translational and Molecular Imaging Institute, Mount Sinai School of Medicine, One Gustave L. Levy Place, Box 1234, New York, New York 10029, United States

[§]SUNY Health Science Center at Brooklyn, Anatomy & Cell Biology, Box 5, 450 Clarkson Avenue, Brooklyn, New York 11203, United States

Supporting Information

ABSTRACT: We have previously reported enhancing the imaging of atherosclerotic plaques in mice using reconstituted high density lipoproteins (HDL) as nanocarriers for the MRI contrast agent gadolinium (Gd). This study focuses on the underlying mechanisms of Gd delivery to atherosclerotic plaques. HDL, LDL, and VLDL particles containing Gd chelated to phosphatidyl ethanolamine (DTPA-DMPE) and a lipidic fluorophore were used to demonstrate the transfer of Gd-phospholipids among plasma lipoproteins *in vitro* and *in vivo*. To determine the basis of this transfer, the roles of phospholipid transfer protein (PLTP) and lipoprotein lipase (LpL) in mediating the migration of Gd-DTPA-DMPE among lipoproteins were investigated. The results indicated that neither was an important factor, suggesting that spontaneous transfer of Gd-DTPA-DMPE was the most probable mechanism. Finally, two independent mouse models were used to quantify the relative contributions of HDL and LDL reconstituted with Gd-DTPA-DMPE to plaque imaging enhancement by MR. Both sets of results suggested that Gd-DTPA-DMPE originally associated with LDL was about twice as effective as that injected in the form of Gd-HDL, and that some of Gd-HDL's effectiveness *in vivo* is indirect through transfer of the imaging agent to LDL. In conclusion, the fate of Gd-DTPA-DMPE associated with a particular type of lipoprotein is complex, and includes its transfer to other lipoprotein species that are then cleared from the plasma into tissues.

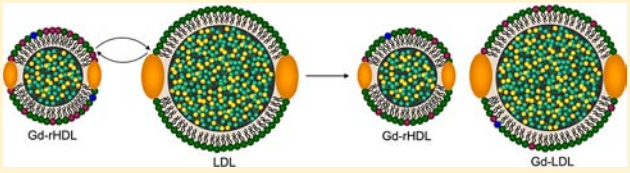

INTRODUCTION

Atherosclerosis is the major underlying cause of coronary artery disease and myocardial infarction.[1] Though other factors also contribute to cardiovascular risk, it has been long appreciated that coronary artery disease is positively linked to plasma levels of low density lipoproteins (LDL). Briefly, LDL particles cross the arterial endothelium, are retained, then modified in the intima of arteries (e.g., see ref 2). Normal and modified LDL can then be taken up by macrophages that are derived from circulating monocytes that infiltrated the arterial wall.[2−4] By this process, macrophages progressively become foam cells, which are the central cellular component of growing plaques. During the process of plaque growth, smooth muscle cells from the arterial media also migrate into the intima, and have the potential to stabilize the atherosclerotic plaque by producing and depositing extracellular matrix components, such as proteoglycans, collagens, tenascin, and fibronectins, particularly in the subendothelium, where a thick fibrous cap forms as a result.[5,6]

In coronary arteries, macrophage-poor atherosclerotic plaques with thick fibrous caps that occlude the majority of the lumen may cause a stable form of myocardial ischemia, or in other sites, cerebral or peripheral vascular disease. Paradoxically, less stenotic plaques, but with high macrophage density and thin fibrous caps, may be responsible for more dangerous coronary artery disease because of a propensity of plaques with these compositional characteristics to rupture.[7−9] A number of imaging approaches have been tried to detect the presence of coronary artery plaques and the risk they impose. Luminography (X-ray angiography or catheterization, an invasive technique) can diagnose luminal narrowing, while electron beam tomography (EBT) and multislice computed tomography (MS-CT) enable the detection of coronary calcification, which, when translated into a summary calcium score, is taken to

Received: February 26, 2013
Revised: April 23, 2013
Published: April 25, 2013

dx.doi.org/10.1021/bc400105j | *Bioconjugate Chem.* 2013, 24, 1039−1048

represent plaque burden and to correlate with disease risk.[10−12] Neither technique, however, can provide information on plaque cellular composition or detect with reliability those plaques that are modestly stenotic, yet still dangerous because their composition and structure predispose them to rupture.

Nanoparticles have been shown to be effective carriers of a wide variety of cargos, including drugs and imaging agents (for recent reviews, see refs 13 and 14). We previously demonstrated in mouse models of atherosclerosis the utility of Gd-DTPA-DMPE incorporated into spherical and discoidal reconstituted high-density lipoproteins (Gd-HDL) to serve as nanocarriers for magnetic resonance imaging (MRI) agents.[15,16] This novel MRI contrast agent proved to be efficient in noninvasively differentiating, with a very high contrast, aortic areas containing atherosclerotic plaques rich in macrophages from nondiseased areas.

The initial success of the Gd-HDL nanoparticles in atherosclerosis imaging stimulated us to investigate their characteristics in more depth. Because it has been known for some time (e.g., see ref 17) that lipids can exchange and transfer between lipoprotein particles in the same density class or in different classes, as well as between lipoproteins and cell membranes, we hypothesized that a Gd-DTPA-DMPE complex incorporated on an HDL nanoparticle has a number of potential carriers into the plaque; for example, on the original or another HDL particle, on a different type of lipoprotein particle (e.g., LDL), or on a plasma protein. We have tested this hypothesis by a variety of *in vitro* and *in vivo* techniques.

MATERIALS AND METHODS

Materials. Gadolinium 1,2-dimyristoyl-*sn*-glycero-3-phosphoethanolamine diethylenetriamine pentaacetic acid (Gd-DTPA-DMPE), and 1,2-dimyristoyl-*sn*-glycero-3-phosphoethanolamine-*N*-(7-nitro-2-1,3-benzoxadiazol-4-yl) (NBD-PE), were all purchased from Avanti Polar Lipids and used as received. Cell culture supplies were purchased from Invitrogen (Carlsbad, CA).

Lipoprotein Isolation and Modification. Very low-density lipoprotein (VLDL) (d < 1.019 g/mL), low-density lipoprotein (LDL) (d 1.019−1.063 g/mL), and high-density lipoprotein (HDL) (d 1.063−1.21 g/mL) were isolated from normal human plasma by sequential density gradient ultracentrifugation. In a typical preparation of modified lipoproteins, a film of phospholipid was formed by evaporation overnight under vacuum of the solvents from a 1:4 methanol:chloroform solution of Gd-DTPA-DMPE and NBD-PE. The film was then rehydrated with the solution of the lipoproteins in prefiltered PBS and 4 cycles of sonication at 0 °C for 1 min followed by a 1 min interval on ice. Purification was achieved by centrifuge filtration and washing numerous times with PBS. The purity of the preparation was confirmed *via* fast protein liquid chromatography (FPLC; details below). The fractions in which native lipoproteins extracted from human plasma, or modified lipoproteins (Gd-VLDL, Gd-LDL, and Gd-HDL), as well as native mouse lipoproteins and plasma proteins, were eluted were approximately fractions 29−38 for VLDL, 39−55 for LDL, 58−67 for HDL, and 68−77 for plasma proteins. The particles were then characterized by dynamic light scattering (DLS), relaxometry, and gadolinium quantification. Characterization of the modified lipoproteins by FPLC and DLS, as well as Gd-HDL capacity to efflux cholesterol from J774 cholesterol loaded cells, afforded clear evidence that the modified material had conserved the expected physical and functional features of the particles before manipulation.

FPLC Analysis. Two Superose-6 FPLC columns in series were pre-equilibrated with buffer (0.15 M NaCl, 1 mM EDTA, pH 7.5). Samples were filtered through a membrane (0.22 μm pore size) to remove any particulate material, and 200 μL aliquots were applied to the columns. The flow rate was 0.3 mL/min, and 0.5 mL fractions were collected. Absorbance of the column effluent at a wavelength of 280 nm was monitored by a UV flow-through detector. The fractions corresponding to the lipoprotein particles noted above were determined by prior analysis of both mouse plasma and the human lipoproteins isolated by density gradient centrifugation.

Dynamic Light Scattering (DLS). The hydrated mean diameters of the different modified lipoprotein preparations were determined by photon correlation spectroscopy performed with a Malvern light scattering instrument (Malvern Instruments, Malvern, UK). All samples were analyzed at 25 °C in filtered water (30 nm size cutoff).

Gadolinium Content and Relaxivity Determinations. Concentrated FPLC fractions were analyzed by inductively coupled plasma mass spectrometry (ICP-MS). The relaxivity measurements were done on a Minispec (Bruker Medical BmbH, Ettingen) operating at 60 MHz and 40 °C.

Phospholipid Transfer Protein Assay. PLTP activity was measured with an assay kit (Cardiovascular Targets Inc., New York, NY, USA) provided by Dr. Xian-Chen Jiang.[18] Briefly, the kit includes donor and acceptor particles, which are incubated with 3 μL of plasma. Fluorescent phospholipid is present in the donor particle in a self-quenched state. The plasma mediates transfer of fluorescent phospholipid *via* PLTP. The transfer due to PLTP is determined by the increase in fluorescence intensity as the fluorescent lipid is removed from the donor and transferred to the acceptor. The PLTP activity assay was validated through comparison by the classic radiolabeled method.[19,20]

Animal Protocols. All procedures were approved by the Animal Care and Use Committees at NYU School of Medicine and the Mount Sinai School of Medicine. The ApoE knockout (KO) mice (C57BL/6 background) used in the experiments were an average of 6 months of age. They were weaned at 1 month and fed a modified high-fat diet (HFD) containing 19.5% fat and 0.3% cholesterol (Dyets Inc., Bethlehem, PA) for 18 weeks. The HFD is higher in fat and cholesterol than a normal (low-fat) chow diet and accelerates formation of atherosclerosis in ApoE KO mice.[21]

The LDL receptor KO animals were also fed the modified Western-type diet (high-fat diet, HFD) for 22 weeks, then the MRI scan in the high endogenous LDL level condition was performed, and the diet switched to the normal chow diet (low-fat diet, LFD) for 2 weeks, after which a new scan was performed for a lower endogenous LDL level condition. On high fat diet feeding, LDL receptor KO mice show highly elevated plasma cholesterol and the development of atherosclerosis.[22] The morphology of the lesions in LDL receptor KO mice is comparable to that in ApoE KO mice, with the plaques developing in a time-dependent manner, starting from the proximal aorta. Unlike the ApoE KO mouse, however, without the high fat diet, atherosclerosis essentially does not progress.[23,24] The ApoA-I KO mice used for an aortic transplant study to examine the effects of a low endogenous level of HDL were fed a low-fat diet. ApoA-I KO mice do not

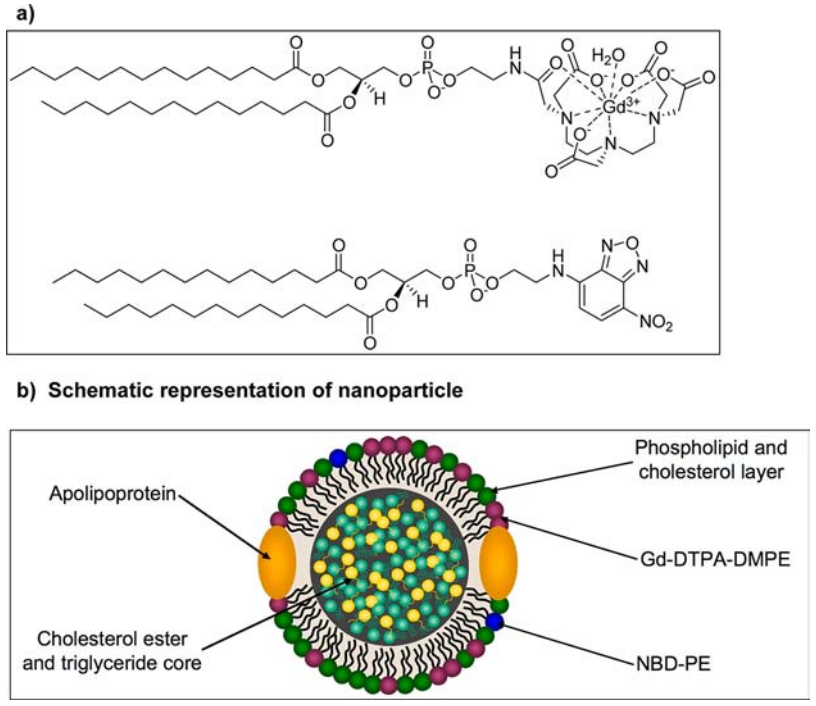

Figure 1. Modified phospholipids integrated in HDL, LDL, and VLDL nanoplatforms via sonication: (a) chemical structures of Gd-DTPA-DMPE and NBD-PE; (b) schematic representation of Gd-HDL particle.

develop significant atherosclerosis even when fed a high-fat, high-cholesterol diet.[25]

Aortic Transplantation. The aortic arch transplantation model has been described elsewhere.[26−28] Briefly, ApoE KO (C57BL/6) mice were weaned at 1 month onto HFD, which was continued for 18 weeks, to become donors of aortic arch segments. The recipients were age-matched ApoA-I KO mice, maintained on standard chow diet. During the transplant, a donor arch was interpositioned with the abdominal aorta in the recipient mouse and blood flow was directed through the graft. The mice were then monitored for 24 h after the transplant, prescanned, injected *via* tail vein with the contrast agent, and reimaged at the 24 h time point (corresponding to 48 h after transplant).

MR Imaging. *In vivo* MRI was performed using a 9.4 T, 89 mm bore MRI system (Bruker Instruments, Billerica, MA). An *in vivo* probe (Micro 2.5, Bruker Instruments) was used in combination with a gradient system of 1000 mT/m and a rise time of 110 ms. The animals were anesthetized with a 4% isoflurane/O_2 gas mixture (400 cc/min initial dose) and maintained with a 1.5−2.0% isoflurane/O_2 gas mixture (100 cc/min maintenance dose) delivered through a nose cone and placed in a 30 mm birdcage coil with an animal handling system. A respiratory sensor connected to a monitoring and gating system (SA Instruments, Stony Brook, NY) was placed on the abdomen to monitor the rate and depth of respiration. A constant body temperature of 37 °C was maintained using a thermocoupler/heating system. The abdominal aorta was identified in a coronal section on a localizing sequence. MRI was performed using a T1-weighted (T1W), black blood sequence. Twenty-two contiguous 500-μm-thick slices with a microscale in-plane resolution of 101 μm were acquired using a spin echo sequence with a 256 × 256 matrix size. The repetition time (TR) and echo time (TE) for the T1W images were 800 and 8.6 ms, respectively. An inflow saturation band of 3 mm was used with a slice gap of 3 mm for additional luminal flow suppression. Sixteen signal averages were used for a total imaging time of 55 min per scan. A saturation pulse was used to eliminate signal from fat tissue and better delineate boundary of the aortic wall and minimize chemical shift artifacts. After a preinjection baseline MRI scan, mice were injected, *via* a tail-vein catheter. Subsequent scans were carried out at 4, 24, 48, and 72 h postinjection.

Use of the medical image analysis software package *eFilm* allowed the MR signal intensity of various tissues from the different time points to be ascertained and the percent change in normalized enhancement ratio (% NER) postinjection to be calculated. Normalization of the MR signal intensity in the aorta wall was performed by rebasing with the signal from the adjacent muscle to create the value *W*. The % NER was found from the difference between *W* from the postinjection scans and *W* from the prescan divided by *W* from the prescan and multiplied by 100, as per the method described in ref 29.

In Vitro Plasma Transfer. Blood was collected from ApoE KO mice by retro-orbital bleeding under anesthesia using heparinized capillary tubes. The blood was collected in microcentrifuge tubes containing EDTA; the plasma was then separated by centrifugation. 200 μL of plasma was incubated at 37 °C for 15 min, 4 h, or 24 h with a solution of the modified lipoproteins containing 15 μmol of Gd (as in Gd-DTPA-DPME). After the incubation time, the solution was filtered through a Millipore sterile filter (0.22 μm cut off) and the various lipoprotein fractions separated by FPLC gel filtration. Each fraction was then collected and analyzed to determine total cholesterol content and fluorescence.

In Vivo Plasma Transfer. ApoE KO mice were injected under anesthesia using a 1 cc syringe to penetrate the retro-orbital sinus with a solution of the modified lipoproteins containing 50 μmol/kg of Gd (as Gd-DTPA-DPME). After the 15 min, 4 h, and 24 h incubation time, blood was collected at

dx.doi.org/10.1021/bc400105j | *Bioconjugate Chem.* 2013, 24, 1039−1048

time of sacrifice by heart puncture under anesthesia into centrifuge tubes containing EDTA and immediately spun down, the plasma filtered through a Millipore sterile filter (0.22 μm cut off), and the various lipoprotein fractions separated by FPLC gel filtration. Each fraction was then collected and the content analyzed to determine total cholesterol content, fluorescence, and Gd content. All ICP-MS measures to determine the Gd content were performed by Cantest Ltd., Burnaby, Canada (now Maxxam Analytics).

Statistics. The typical data are mean ± SEM based on n = 3−5 for each observation.

RESULTS AND DISCUSSION

Gd-HDL is an effective imaging agent platform,[15,16] but its interactions with other blood components and the molecular mechanisms by which contrast generating material is delivered to atherosclerotic plaques are unknown. Because phospholipid transfer or exchange among lipoproteins and other amphiphile based species, such as liposomes, is a well-known phenomenon (e.g., ref 17), we tested whether some of the Gd, which is chelated to a group covalently attached to phosphoethanolamine (PE), could be transferred from the particle in which it is originally integrated to other lipoproteins or to plasma proteins. If so, this would imply that there are at least 2 routes by which the HDL-associated Gd that enhances plaque imaging[16] could enter the arterial wall: directly on the original particle or indirectly on either another lipoprotein or a plasma protein after transfer from the original particle.

Properties of the Tested Gd-Lipoproteins. For tests of the transfer of Gd, we designed a series of nanoparticles incorporating the Gd-phospholipid moiety into HDL, LDL, or VLDL that had been isolated by ultracentrifugation from human plasma. In these particles (Figure 1), the metal ion is chelated in a phospholipid molecule with a C-14 lipidic chain (Gd-DTPA-DMPE), while the fluorescent probe NBD is bound to the analogue nonchelating phospholipid and exposed to solvent (NBD-PE). These particles resemble those used in previous imaging studies (e.g., refs 15 and 30) and in the present experiments were subjected to transfer assays conducted *in vitro* and *in vivo* (see below).

The release of free Gd^{3+} ions from gadolinium-based contrast agents is a current concern due to the reports of nephrogenic systemic fibrosis following their use.[31] Furthermore, should there be significant release of Gd^{3+} from the chelates in the experimental time frame, this could have marked effects on our results. Therefore, we used the xylenol orange assay[32] to determine whether Gd^{3+} was released from our agent *in vitro* or *in vivo* (SI Figure S1). First, we incubated Gd-HDL in serum for 24 h at 37 °C. We observed no release of Gd^{3+} compared to nonincubated Gd-HDL, indicating the stability of our formulation (SI Figure S1b). Next, we injected three mice with Gd-HDL at a dose of 50 μmol Gd/kg. At 4 h postinjection (the typical time point used for the lipoprotein transfer experiments), plasma samples were acquired. ICP-MS analysis determined the average Gd content of plasma to be 169 μM. The free Gd^{3+} content was below the sensitivity of the xylenol orange experiment (<1 μM, SI Figure S1c). Therefore, the free Gd^{3+} was less than 1% of the total, indicating that release of Gd from the chelate is not a confounding factor in this experiment.

We also physically characterized the Gd-enriched lipoproteins after incorporation of the Gd-phospholipid in relation to the known properties of the starting (native) particles.[33] The apparent hydrodynamic diameters of the particles from multiple preparations as determined by light scattering are reported in Table 1, and showed no noticeable changes from native particles, which are VLDL (30−80 nm), LDL (22 nm), HDL_2 (12 nm), HDL_3 (8.5 nm);[33,34] moreover, FPLC elution profiles of the modified lipoproteins confirmed these observations (data not shown). The longitudinal relaxivities (r_1) of the nanoparticles were measured on a 60 MHz Bruker Minispec at 40 °C, and did not differ substantially from our previously reported preparations of Gd-HDL.[15,16] A trend toward lower values of r_1 can be noticed with increasing diameter of the particle (Table 1).

Table 1. Characterization of Particles Incorporating Gd-DTPA-DMPE and NBD-PE: Mean Diameters in Aqueous Solution, As Determined by Light Scattering, And Longitudinal Relaxivity (r_1), Measured on a 60 MHz Bruker Minispec at 40 °C

particle	diameter (nm)	r_1 (mM^{-1} s^{-1})
Gd-HDL	9.18 ± 1.78	10.9 ± 1.3
Gd-LDL	21.86 ± 3.18	9.9 ± 1.2
Gd-VLDL	38.63 ± 2.64	9.9 ± 1.2

Sonication of proteins, if performed for extensive periods of time and at high temperatures, may cause protein inactivity because of misfolding or aggregation.[35] In order to verify the lack of effects of the sonication procedure on the general activity of the Gd-HDL, the cholesterol efflux capacities of the starting material HDL and the modified Gd-HDL particles were compared to that of a standard subfraction of HDL (HDL_3) in cholesterol-loaded J774 macrophage cells. No significant differences were observed, with starting HDL and modified Gd-HDL supporting approximately the same amount of cholesterol efflux that occurred with fresh HDL_3 (~5% over 4 h, data not shown). These tests confirmed that the low-intensity sonication method used for the incorporation of the Gd-phospholipid did not cause major changes in the physical properties of the lipoproteins, and, for Gd-HDL, in its cholesterol efflux potential.

Analogously, preservation of the functional properties of Gd-LDL after sonication was verified by cellular uptake experiments with Gd- and fluorescent-labeled LDL using HepG2 cells with and without native LDL competition. As a consequence of the competition, uptake after 2 h was reduced for both the Gd-containing fluorescently labeled LDL (by 59.7%) and the fluorescently labeled LDL (by 45.4%), proving that the binding of the particles to the LDL receptor is specific and that the reconstituted LDL is biologically active (SI Figure S2).

Finally, native human VLDL was compared with Gd-VLDL, in order to assess the effect of sonication on its apolipoprotein composition. Gel electrophoresis indicated no significant change in the protein profile after the sonication procedure, particularly with regard to the contents of the LDL receptor ligands apolipoproteins B and E, indicating that VLDL was unchanged (SI Figure S3).

Transfer of Phospholipids among the Gd-Lipoproteins *in Vitro*. Two likely possibilities of transferring the Gd-DTPA-DMPE imaging payload from HDL to another phospholipid surface (such as to another lipoprotein particle) are spontaneous or phospholipid transfer protein (PLTP)-mediated transfers. The consequence of such transfers would be the separation between the initial delivery vehicle and the payload. Our initial approach to study transfer of the Gd-

DTPA-DMPE from Gd-HDL was to establish an *in vitro* system in which the movement of the fluorescently labeled phosphoethanolamine (NBD-PE) incorporated into the lipoproteins was used as a surrogate for the Gd-DTPA-DMPE. Note that studies *in vivo*, presented below and in Figures 5 and 6, as well as SI Figures S7−9, support that the movement of NBD reasonably matched that of Gd.

In the first set of experiments, we studied Gd-DTPA-DMPE and the fluorescent phospholipid NBD-PE incorporated into HDL, LDL, or VLDL. The *in vitro* incubation of each of the Gd- and NBD-containing lipoproteins at 37 °C for 15 min, 4 h, and 24 h with fresh plasma pooled from ApoE-deficient (ApoE KO) mice, a common model of atherosclerosis previously used in our imaging studies, revealed transfer of the fluorescent label to other classes of endogenous lipoproteins (Figure 2 reports

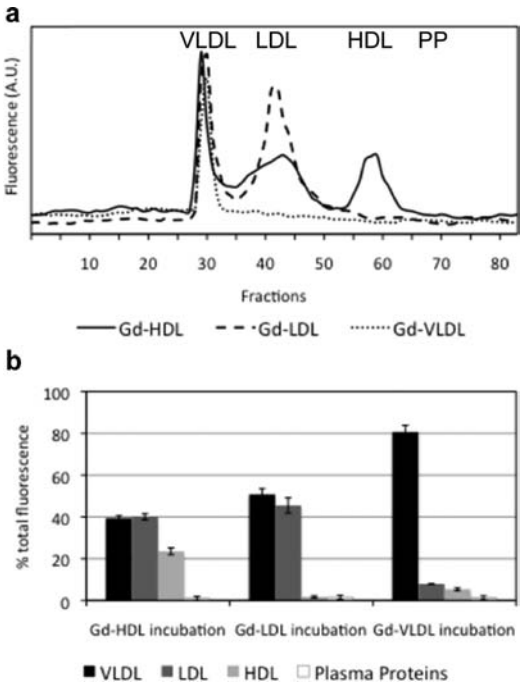

Figure 2. (a) Fluorescence curves and (b) graphs of fluorescence distribution after 4 h *in vitro* incubation of ApoE KO mice plasma with human lipoproteins carrying Gd-DTPA-DMPE and NBD-PE (n = 5). Note that the Gd-HDL particle transfers its fluorescent NBD-PE to endogenous LDL and VLDL (continuous line). Gd-LDL can transfer the fluorescent label to VLDL, but not to HDL (dashed line). Gd-VLDL is incapable of transferring the fluorophore to any of the endogenous lipoproteins (dotted line). Transfer to plasma proteins was not detected.

data for the 4 h *in vitro* incubation time). Interestingly, the transfer was preferentially directed according to density, i.e., the fluorescent label went generally from particles of higher to lower density. From HDL, 41% and 39% of the fluorescent label appeared in LDL and VLDL, respectively, by 4 h. Similarly, if the labeled material was initially incorporated into LDL, there was 48% transfer to VLDL. In contrast, in all experiments, transfer to smaller lipoproteins of fluorescent label originating in larger ones was negligible. Also, there was no apparent transfer to the plasma proteins, which elute on the FPLC columns at higher retention times relative to HDL.

In order to determine whether the observed preferential direction of transfer was associated with the nature of the particles themselves, or a reflection of the relatively higher content of LDL and VLDL particles in ApoE KO plasma compared to HDL, a similar *in vitro* experiment using human plasma (higher in HDL content compared to ApoE KO mouse plasma; i.e., 60 mg/dL vs 27 mg/dL) was performed. It revealed that incubation with Gd-HDL led to transfer to LDL and VLDL (Figure 3), though to a lesser extent than in mouse

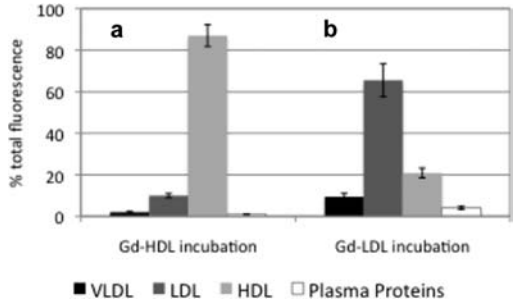

Figure 3. Distribution of fluorescence after 4 h *in vitro* incubation of human plasma with (a) Gd-HDL carrying Gd-DTPA-DMPE and NBD-PE (n = 3); and (b) Gd-LDL carrying Gd-DTPA-DMPE and NBD-PE (n = 3). For both incubations, there is transfer of the fluorescent label from the donor particles to the other classes of lipoproteins. In particular, in (b), note the Gd-LDL transfer to HDL.

plasma (Figure 2). Furthermore, incubation of Gd-LDL promoted an enrichment in fluorescence of both HDL and VLDL. Therefore, the predominant transfer of label from higher to lower density lipoproteins in Figure 2 may reflect the relative concentrations of the different lipoprotein species, which in ApoE KO mice are heavily biased toward VLDL and VLDL remnant-like particles, or in intrinsic differences between human and mouse lipoproteins or in other plasma components.

Mechanism of Transfer of Phospholipids among the Lipoproteins *in Vitro*. In order to explain the basis for transfer, we considered two well-known mechanisms from the field of lipoprotein metabolism, namely, PLTP-mediated and spontaneous transfer. PLTP is a 476 amino acid secreted protein that catalyzes the transfer of phospholipids and vitamin E among lipoprotein particles. PLTP plays a key role in the formation and homeostasis of high-density lipoprotein particles; it has been studied mainly in regard to transferring phospholipids from VLDL lipoprotein surface remnants to HDL particles,[36] but it also has the ability to mediate more general phospholipid transfers among the different lipoprotein classes.[37,38] In spontaneous transfers, the rate-limiting step is desorption of the lipid from the donor surface into the aqueous phase.[39] Decreasing donor particle size, and hence increasing surface curvature, then, would be expected to accelerate loss of phospholipids through spontaneous transfer.

On the other hand, *in vitro* PLTP-mediated transfer occurs through protein and lipoprotein bi- or trimolecular collisions, and it was shown to be dependent on the nature of the acceptor as well as on concentrations of acceptor and donor.[40] In particular, the highest rate of transfer mediated by PLTP occurs when HDL is utilized as donor. This implies that when using HDL or other lipoproteins to deliver therapeutic or diagnostic agents loaded on the surface, PLTP has the potential to distribute these agents to endogenous lipoproteins.

In order to test whether PLTP has this potential for NBD-PE transfer from Gd-HDL, the *in vitro* experiments were repeated with the addition of a PLTP-specific inhibitor. The inhibitor (a gift from Dr. Changbin Guo, Capital Normal University,

dx.doi.org/10.1021/bc400105j | *Bioconjugate Chem.* 2013, 24, 1039−1048

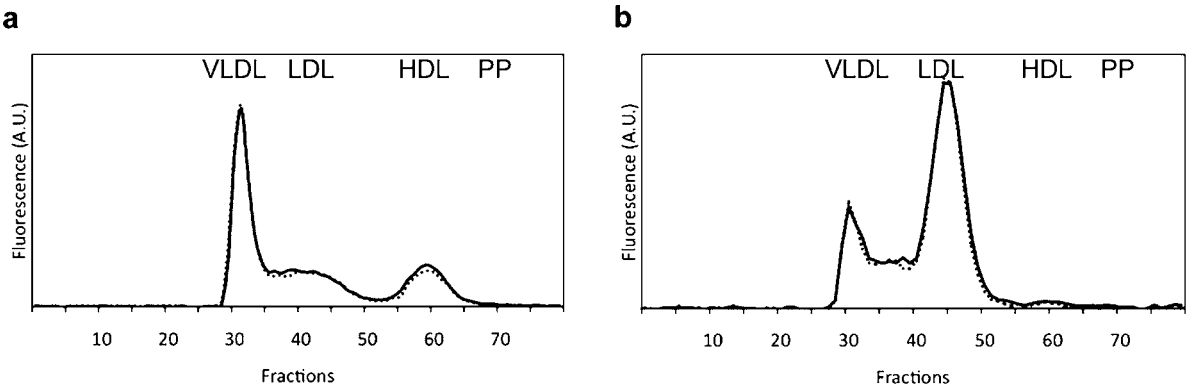

Figure 4. Four hour *in vitro* incubation of ApoE KO mouse plasma with (a) human HDL carrying Gd-DTPA-DMPE and NBD-PE; or (b) human LDL carrying Gd-DTPA-DMPE and NBD-PE, in the presence (continuous line, $n = 2$) or absence (dotted line, $n = 2$) of a specific PLTP inhibitor. No significant change in the fluorescence profiles are evident.

Beijing, China) is designated as #40 and its IC_{50} is 15 μM. The inhibitor was added to fresh ApoE KO mouse plasma containing either the Gd-HDL or Gd-LDL particles. The concentration of compound #40 (75 μM) was chosen to result in 100% inhibition of PLTP, as confirmed by finding no significant difference in transfer activity between samples of plasma from a PLTP KO mouse and from an ApoE KO mouse to which the compound was added (SI Figures S4 and S5). As evident in Figure 4, the transfer profiles of plasma lipoproteins from experiments conducted in the presence of the PLTP-inhibitor differ little from the ones performed without the inhibitor, and there is no evidence of any diminished transfer capacity due to the presence of the inhibitor. There was also no evidence that another lipase that remodels lipoproteins, lipoprotein lipase, was responsible for transfer (SI Figure S6). These observations suggest that, at least for the *in vitro* experiments, the most probable mechanism of transfer of the Gd-DTPA-DMPE surrogate is the spontaneous desorption of phospholipids from the reconstituted particles and subsequent association with the plasma lipoproteins.

Transfer of Phospholipids among the Gd-Lipoproteins *in Vivo*. In the second set of experiments, ApoE KO mice were injected with Gd-HDL, Gd-LDL, or Gd-VLDL as Gd-DTPA-DMPE. After 15 min, 4 h, or 24 h, the animals were sacrificed, the plasma lipoproteins separated *via* FPLC, and cholesterol content and fluorescence measured in each fraction. Analogous to the *in vitro* experiments, the fluorescent label from the original lipoprotein carrier was now found in other classes of lipoproteins of lower density (Figure 5 and SI Figure S7). For example, as shown in Figure 5, from HDL, 35% and 51% of the fluorescent label was found with LDL and VLDL, respectively, by 4 h; from LDL, 50% was now with VLDL. Compared to the experiments *in vitro*, there was also little fluorescence found in the higher density lipoproteins when lower density carriers were injected. For example, at 4 h, when Gd-LDL was injected, 4% was found with HDL, and when Gd-VLDL was injected, 22% was found with LDL (Figure 5b,c). As before, none of the experiments showed the appreciable appearance of fluorescence in the plasma proteins.

Note that because under the conditions *in vivo*, unlike *in vitro*, there is clearance of lipoproteins, the distribution of fluorescence after injection reflects not only transfer, but also the plasma residence time of the lipoprotein species. Given the differences in plasma half-lives (HDL > LDL > VLDL; reviewed in ref 33), the quantitative impact of clearance on the fluorescence associated with the species of lipoprotein will vary. Nonetheless, with the plasma half-life of LDL being at least one day,[41] and that of HDL being even longer, the loss of fluorescence from the injected HDL or LDL at 15 min or 4 h cannot be explained by clearance of the particles, and must represent transfer.

In order to address the possibility that the distribution of the NBD fluorophore might not reflect the behavior of Gd, the concentrations of Gd in the eluted lipoprotein fractions obtained from the *in vivo* mixing experiments were directly measured *via* ICP-MS at the 4 and 24 h time points (Figure 6 and SI Figure S8). Even though the graphs in Figures 5 and 6 are not superimposable, the results showed reasonably similar trends in the distributions of the Gd and NBD, namely, that the majority of either fluorescence or Gd was no longer associated with the injected Gd-HDL by 4 h, a time point at which most of the injected particles would be expected to remain in the circulation (supported by finding in the ICP-MS assays that the Gd content of the plasma decreased by only ~30% at 4 h). This loss of either the fluorescence or Gd from the Gd-HDL particles was also observed *in vitro* (Figures 2, 3, 4; and SI Figures S6, S9) in which lipoprotein clearance could not have been a factor. In the aggregate, the data *in vitro* and *in vivo* (Figures 2–6; SI Figures S6–9) also suggest that the NBD-phospholipid probe is a useful, if not exact (likely due to the structural and charge differences of what is attached to the PE), surrogate for the behavior of the Gd-carrying phospholipids, with the significant advantage of avoiding the relatively high cost of ICP-MS assays.

That both types of experiments (*in vitro* and *in vivo*) provided evidence that Gd-bearing phospholipids were transferred among the different classes of lipoproteins is consistent with the transfer phenomena that occur for natural phospholipids (e.g., refs 42–44 and 17). This implies that transferring behavior, as well as clearance characteristics, need to be taken into consideration when designing a lipoprotein-based imaging or therapeutic agent, or when interpreting the results from their use. For example, transfer can cause loss of efficiency of the imaging agent if it were transferred to a particle either incapable of entering the vessel wall or so rapidly cleared from plasma that it has little opportunity to enter the target tissue of interest.

Imaging Studies. The different Gd-containing particles were also injected into ApoE KO mice to test their imaging enhancement of aortic atherosclerotic plaques. The normalized

dx.doi.org/10.1021/bc400105j | *Bioconjugate Chem.* 2013, 24, 1039–1048

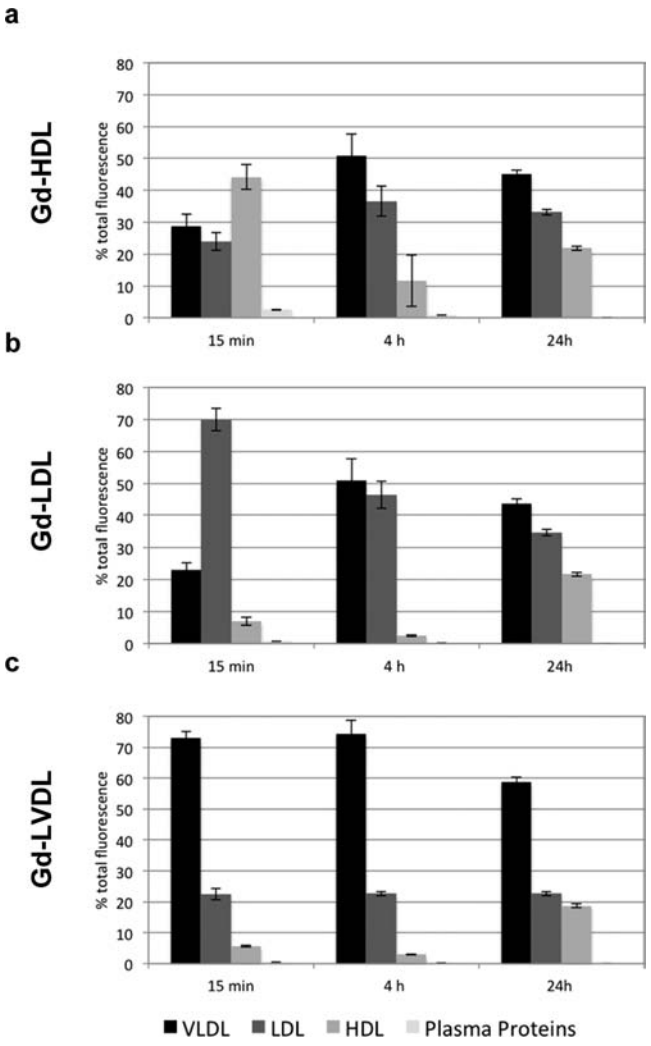

Figure 5. Fluorescence label distribution from ApoE KO mice plasma 15 min, 4 h, and 24 h after injections of mice with human lipoproteins HDL, LDL, and VLDL carrying Gd-DTPA-DMPE and NBD-PE. (a) The incubation with Gd-HDL (n = 3) shows association with endogenous lipoproteins already after 15 min. (b) After injection of Gd-LDL (n = 3), fluorescent label appears in VLDL, analogous to the *in vitro* transfer experiments. Note also that, in contrast to the *in vitro* transfer, a slightly higher appearance of fluorescence in endogenous HDL was observed. (c) The incubation with Gd-VLDL (n = 3) shows appearance of fluorescence in endogenous LDL and a smaller amount in HDL. Interestingly, little fluorescence is seen in the plasma proteins *in vivo* after injection of any of the lipoproteins.

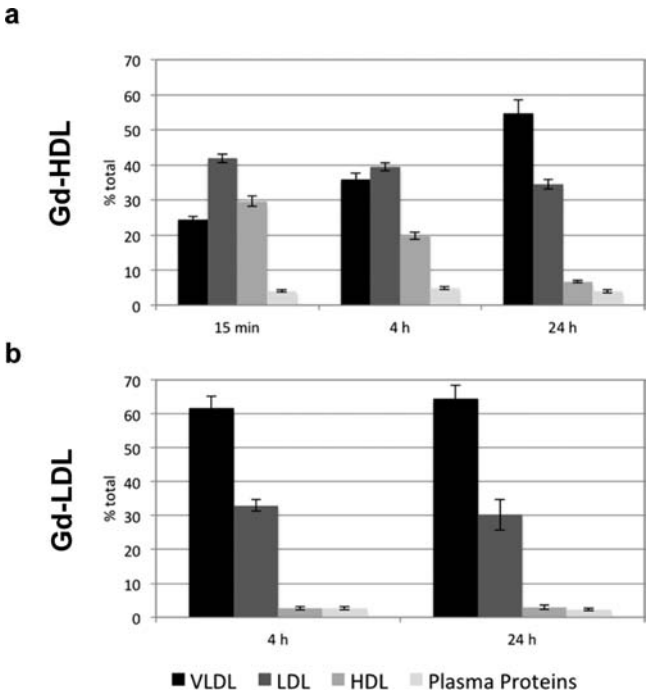

Figure 6. Distribution of Gd in FPLC fractions measured by inductively coupled plasma mass spectrometry (ICP-MS). The plasma was collected from ApoE KO mice that were injected with a 50 μmol/kg dose of Gd as in Gd-DTPA-DMPE integrated in human lipoproteins and sacrificed after 15 min, 4 h, or 24 h after HDL (a) or LDL (b) injections.

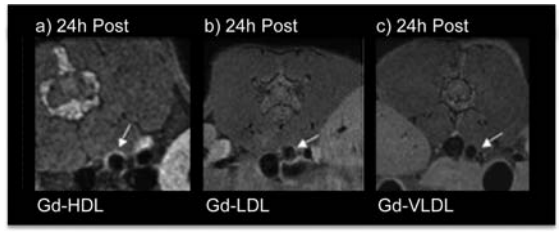

Figure 7. Representative MR images of ApoE KO mouse aorta 24 h after injection of 50 μmol Gd/kg. Injected were (a) Gd-HDL (n = 3), (b) Gd-LDL (n = 3), and (c) Gd-VLDL (n = 3), enriched with Gd-DTPA-DMPE and NBD-PE. The arrows indicate the aorta and the most significant enhanced areas.

enhancement ratios (NER) at 24 h postinjection with respect to muscle (control tissue) for the Gd-HDL, Gd-LDL, and Gd-VLDL particles (containing 50 μmol/kg Gd as Gd-DTPA-DMPE, n = 3 for each particle) were 69 ± 19%, 54 ± 16%, and 9 ± 8%, respectively (given as the mean ± the standard deviation) (representative images are shown in Figure 7).

In order to deliver their Gd cargo to plaques, the associated lipoproteins must enter and accumulate in the intima of arteries. This accumulation is dependent on the balance between the rates at which they enter and leave the arterial wall, as well as on their degradation within the plaque. Studies in humans, rabbits, and pigs suggest that influx of lipoproteins into the intima increases directly with increasing lipoprotein concentration in plasma and decreases inversely with increasing lipoprotein diameter.[45−48] Very large lipoproteins seem to be excluded from the intima,[49] consistent with the relatively poor NER with VLDL, despite its being an excellent acceptor for the Gd-phospholipid in the transfer experiments. In addition to its size, another contributing factor working against VLDL being an effective carrier of Gd into the arterial wall is its aforementioned rapid clearance from plasma. For these reasons, Gd-VLDL was not further utilized for MR experiments.

Relationship between the Levels of Endogenous Lipoproteins and Imaging Enhancement. Although the above results showed modestly better imaging enhancement with Gd-HDL vs Gd-LDL, it was not clear whether the results were influenced by the levels of endogenous lipoproteins, which among other effects, would include changing the degree of transfer, based on the comparison between the data in Figures 2 and 3. To address this issue, in one approach a variation of the well-established aortic arch transplant method we have established for studies of atherosclerosis regression in ApoE KO mice was utilized.[26−28] With this technique, the plasma

dx.doi.org/10.1021/bc400105j | *Bioconjugate Chem.* 2013, 24, 1039−1048

lipoprotein environment to which a plaque is exposed can be rapidly changed and sustained. In the second set of studies, we used a dietary approach in which the lipoprotein profile of LDLr KO mice can be changed within a relatively short time (two weeks).

For the transplant study, ApoE KO mice were fed for 18 weeks a high fat, high cholesterol diet. These conditions result in a substantial amount of plaque in arches and descending aortas. Arches from those animals were then transplanted into the aortae of ApoA-I KO mice[25] of matched age, which have no detectable plasma apolipoprotein A-I, very low levels of HDL particles, and a total plasma cholesterol level reduced to about one-third of wild type mice. In spite of these changes, plaques do not regress.[50] The average total cholesterol level of the ApoA-I KO mice recipients was 44 mg/dL (mean value for 4 animals), in agreement with previous literature.[51] Twenty-four hours after transplant, the mice were prescanned and injected with a 50 μmol Gd/kg dose of either the Gd-HDL or Gd-LDL nanoparticles, and the scan repeated 24 h after injection.

The very small pool of endogenous lipoproteins present in the transplant recipients gives an almost negligible possibility of transfer from the injected lipoprotein, allowing the direct attribution of any enhancement to the Gd on the injected lipoprotein. The NER for the Gd-HDL (n = 3) and Gd-LDL (n = 3) injections were, respectively, 33 ± 4% and 61 ± 11% (Figure 8). In comparison to the contrast enhancement observed in ApoE KO mice, these results suggest that a reasonable amount of the imaging efficacy of the HDL could be explained by transfer to endogenous LDL (~50% based on the NER values, but as noted above, this is a semiquantitative estimate because the impact of lipoprotein clearance is not accounted for), with the rest by direct delivery to the plaque. Gd incorporated into LDL, in contrast, appears to be directly delivered to the plaque given the comparable NERs independent of the differences in the plasma lipoprotein profiles.

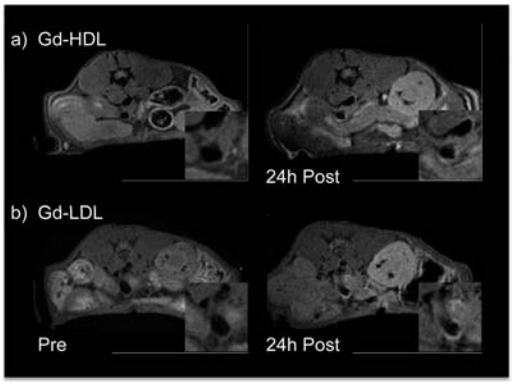

Figure 8. Representative MR images of apoE KO aortic arches transplanted into ApoAI KO mice, pre injection and 24 h after injection of 50 μmol Gd/kg of Gd-HDL and Gd-LDL, enriched with Gd-DTPA-DMPE and NBD-PE.

The second approach used a dietary protocol to further study the imaging capabilities of Gd-HDL in different plasma lipid environments. Total plasma cholesterol levels in LDL-receptor KO mice can be easily manipulated according to diet: on high-fat diet (HFD) their total plasma cholesterol level is about 1500 mg/dL (causing atherosclerosis to develop to an advanced state over the 22 weeks of diet consumption), and decreases to 250 mg/dL if fed for a minimum of 2 weeks the low-fat diet (LFD), with the decrease associated with marked reductions in VLDL, IDL, and LDL cholesterol, and an increase in HDL cholesterol.[22,52] Plaques that develop under the HFD do not regress by 2 weeks after the mice are switched to LFD (C. Yuan, E. Fisher, unpublished). Into these two plasma lipid environments (i.e., HFD, LFD fed LDLR−/− mice), 50 μmol/kg Gd (as Gd-DTPA-DMPE) in Gd-HDL were injected. Calculated enhancement after the Gd-HDL injection went from 89 ± 18% on HFD (i.e., high LDL, low normal HDL endogenous plasma pools) to 47 ± 13% on LFD (i.e., lower LDL, higher HDL endogenous pools). Total cholesterol (C) went from 1500 mg/dL in mice fed HFD to 200 mg/dL in those fed LFD. The ratio of LDL-C/HDL-C went from ~40 in the HFD group to ~1.5 in the LFD group (based on LDL-C in HFD of 330 mg/dL, 115 in LFD; HDL-C of 8 mg/dL in HFD, 75 in LFD) (Figure 9).

Though a very different experimental design from the transplant study, the results again suggest that a significant fraction (~50%) of the Gd on HDL is targeted indirectly to the plaque, most likely by transfer to LDL. In other words, the greater NER on HFD vs LFD, the latter with the significantly higher plasma LDL concentration, likely reflects the transfer of Gd from a lower (i.e., HDL) to a higher (i.e., LDL) efficacy delivery system, so that two delivery vehicles (HDL and LDL) were concurrently operative. A mechanistic basis for an augmentation of HDL's imaging ability by transfer to LDL may be related for the tendency of LDL to be retained in plaques,[2] whereas HDL has a relatively short plaque residence time.[53,54]

CONCLUSION

We previously showed that HDL could be adapted for the noninvasive imaging of atherosclerotic plaques by incorporating

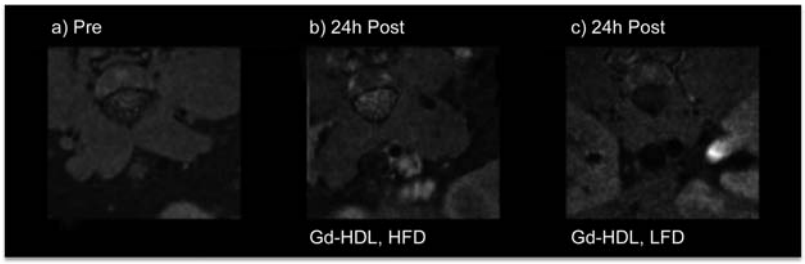

Figure 9. Representative MR images of LDLR KO mouse aortas 24 h after injection of 50 μmol Gd/kg of Gd-HDL enriched with Gd-DTPA-DMPE and NBD-PE. Mice had total endogenous cholesterol levels of about 1500 mg/dL on high-fat diet (HFD, n = 4) (b), or 250 mg/dL in low-fat diet (LFD, n = 4) (c). The same animal was injected at 2 weeks time after the diet shift and is shown here.

Gd-DTPA-DMPE into the phospholipid surface of the lipoprotein (e.g., refs 15,16). In the present report, we have extended those studies by exploring the fate of the imaging agent after it is exposed to the plasma environment. In particular, the possibility of phospholipid transfer from the Gd-bearing nanoplatform to the different classes of lipoproteins and the plasma proteins was assessed by approaches *in vitro* and *in vivo*. Multiple lines of evidence pointed to the migration of the Gd-phospholipid moiety from HDL to native LDL and VLDL. There could also have been transfer to other HDL particles, with subsequent transfer to the LDL and VLDL particles, but this would not have been distinguished from direct transfer from HDL in the assays.

The mechanism of transfer was independent of the activity of phospholipid transfer protein and lipoprotein lipase, and most likely was due to spontaneous desorption driven by the relative differences in the concentrations of the different lipoprotein classes. Interestingly, when Gd-DTPA-DMPE was incorporated into LDL, the plaque imaging efficacy was even greater than that of Gd-HDL, which would explain why delivery of Gd on HDL is still an effective imaging agent even if a fraction of it is transferred to LDL.

In conclusion, HDL nanoplatforms carrying contrast media are powerful agents for high-resolution MR imaging techniques. They are particularly attractive for a number of reasons: ease of preparation and reconstitution; biocompatibility; atheroprotective properties; possibility of loading material both on the phospholipid layer and in the lipophilic core. The present studies point out the complexity of the fate of imaging agents associated as a modified phospholipid with HDL, which includes transfer to other lipoproteins, as well as clearance from the plasma along with its carrier particle. Overall, the present results represent a significant advance in understanding how HDL reconstituted with Gd-DTPA-DMPE functions as an effective atherosclerosis imaging agent.

■ ASSOCIATED CONTENT

Supporting Information

Additional figures as described in text. This material is available free of charge via the Internet at http://pubs.acs.org.

■ AUTHOR INFORMATION

Corresponding Author

*E-mail: edward.fisher@nyumc.org.

Present Address

Alessandra Barazza, Bristol-Myers Squibb, Process R&D, One Squibb Drive, New Brunswick, NJ 08903.

Notes

The authors declare no competing financial interest.

■ ACKNOWLEDGMENTS

We are grateful to Dr. Sajesh Parathath (NYU School of Medicine) for his contribution in the efflux studies, to Dr. Jonathan E. Feig (NYU School of Medicine) for providing the ApoA-I-deficient animals, as well as to all the members of Dr. Fisher's and Dr. Fayad's groups for helpful discussions. We thank Dr. Changbin Guo (Capital Normal University, Beijing, China) for the generous donation of the PLTP inhibitor, and Dr. Brenda Sanchez-Gaytan for her help with the Xylenol orange experiments. We are also thankful to Dr. Michael Phillips and Dr. Kevin J. Williams for their contributions to study design and interpretation. These studies were supported by NIH grants EB 009638, HL 084312, HL 098055, and EB 012165.

■ REFERENCES

(1) Fuster, V., Voute, J., Hunn, M., and Smith, S. C., Jr. (2007) Low priority of cardiovascular and chronic diseases on the global health agenda: a cause for concern. *Circulation 116*, 1966−70.

(2) Williams, K. J., and Tabas, I. (1995) The response-to-retention hypothesis of early atherogenesis. *Arterioscler. Thromb. Vasc. Biol. 15*, 551−61.

(3) Lusis, A. J. (2000) Atherosclerosis. *Nature 407*, 233−41.

(4) Williams, K. J., and Tabas, I. (2005) Lipoprotein retention–and clues for atheroma regression. *Arterioscler. Thromb. Vasc. Biol. 25*, 1536−40.

(5) Wagner, W. D. (1985) Proteoglycan structure and function as related to atherosclerosis. *Ann. N.Y. Acad. Sci. 454*, 52−68.

(6) Libby, P. (2000) Changing concepts of atherogenesis. *J. Intern. Med. 247*, 349−58.

(7) Davies, M. J., and Thomas, A. (1984) Thrombosis and acute coronary-artery lesions in sudden cardiac ischemic death. *N. Engl. J. Med. 310*, 1137−40.

(8) Fuster, V., Stein, B., Ambrose, J. A., Badimon, L., Badimon, J. J., and Chesebro, J. H. (1990) Atherosclerotic plaque rupture and thrombosis. Evolving concepts. *Circulation 82*, II47−59.

(9) Maseri, A., and Fuster, V. (2003) Is there a vulnerable plaque? *Circulation 107*, 2068−71.

(10) Arad, Y., Spadaro, L. A., Goodman, K., Lledo-Perez, A., Sherman, S., Lerner, G., and Guerci, A. D. (1996) Predictive value of electron beam computed tomography of the coronary arteries. 19-month follow-up of 1173 asymptomatic subjects. *Circulation 93*, 1951−3.

(11) Gruntzig, A. (1978) Transluminal dilatation of coronary-artery stenosis. *Lancet 1*, 263.

(12) Nieman, K., Oudkerk, M., Rensing, B. J., van Ooijen, P., Munne, A., van Geuns, R. J., and de Feyter, P. J. (2001) Coronary angiography with multi-slice computed tomography. *Lancet 357*, 599−603.

(13) Farokhzad, O. C., and Langer, R. (2009) Impact of nanotechnology on drug delivery. *ACS Nano 3*, 16−20.

(14) Jaffer, F. A., Libby, P., and Weissleder, R. (2007) Molecular imaging of cardiovascular disease. *Circulation 116*, 1052−61.

(15) Frias, J. C., Ma, Y., Williams, K. J., Fayad, Z. A., and Fisher, E. A. (2006) Properties of a versatile nanoparticle platform contrast agent to image and characterize atherosclerotic plaques by magnetic resonance imaging. *Nano Lett. 6*, 2220−4.

(16) Frias, J. C., Williams, K. J., Fisher, E. A., and Fayad, Z. A. (2004) Recombinant HDL-like nanoparticles: a specific contrast agent for MRI of atherosclerotic plaques. *J. Am. Chem. Soc. 126*, 16316−7.

(17) Bell, F. P. (1978) Lipid exchange and transfer between biological lipid-protein structures. *Prog. Lipid Res. 17*, 207−43.

(18) Cavusoglu, E., Marmur, J. D., Chhabra, S., Chopra, V., Eng, C., and Jiang, X. C. (2009) Relation of baseline plasma phospholipid transfer protein (PLTP) activity to left ventricular systolic dysfunction in patients referred for coronary angiography. *Atherosclerosis 207*, 261−5.

(19) Jauhiainen, M., Metso, J., Pahlman, R., Blomqvist, S., van Tol, A., and Ehnholm, C. (1993) Human plasma phospholipid transfer protein causes high density lipoprotein conversion. *J. Biol. Chem. 268*, 4032−6.

(20) Tall, A. R., Krumholz, S., Olivecrona, T., and Deckelbaum, R. J. (1985) Plasma phospholipid transfer protein enhances transfer and exchange of phospholipids between very low density lipoproteins and high density lipoproteins during lipolysis. *J. Lipid Res. 26*, 842−51.

(21) Plump, A. S., Smith, J. D., Hayek, T., Aalto-Setala, K., Walsh, A., Verstuyft, J. G., Rubin, E. M., and Breslow, J. L. (1992) Severe hypercholesterolemia and atherosclerosis in apolipoprotein E-deficient mice created by homologous recombination in ES cells. *Cell 71*, 343−53.

(22) Ishibashi, S., Brown, M. S., Goldstein, J. L., Gerard, R. D., Hammer, R. E., and Herz, J. (1993) Hypercholesterolemia in low

density lipoprotein receptor knockout mice and its reversal by adenovirus-mediated gene delivery. *J. Clin. Invest. 92*, 883−93.
(23) Breslow, J. L. (1996) Mouse models of atherosclerosis. *Science 272*, 685−8.
(24) Sjoland, H., Eitzman, D. T., Gordon, D., Westrick, R., Nabel, E. G., and Ginsburg, D. (2000) Atherosclerosis progression in LDL receptor-deficient and apolipoprotein E-deficient mice is independent of genetic alterations in plasminogen activator inhibitor-1. *Arterioscler. Thromb. Vasc. Biol. 20*, 846−52.
(25) Williamson, R., Lee, D., Hagaman, J., and Maeda, N. (1992) Marked reduction of high density lipoprotein cholesterol in mice genetically modified to lack apolipoprotein A-I. *Proc. Natl. Acad. Sci. U. S. A. 89*, 7134−8.
(26) Chereshnev, I., Trogan, E., Omerhodzic, S., Itskovich, V., Aguinaldo, J. G., Fayad, Z. A., Fisher, E. A., and Reis, E. D. (2003) Mouse model of heterotopic aortic arch transplantation. *J. Surg. Res. 111*, 171−6.
(27) Llodra, J., Angeli, V., Liu, J., Trogan, E., Fisher, E. A., and Randolph, G. J. (2004) Emigration of monocyte-derived cells from atherosclerotic lesions characterizes regressive, but not progressive, plaques. *Proc. Natl. Acad. Sci. U. S. A. 101*, 11779−84.
(28) Trogan, E., Fayad, Z. A., Itskovich, V. V., Aguinaldo, J. G., Mani, V., Fallon, J. T., Chereshnev, I., and Fisher, E. A. (2004) Serial studies of mouse atherosclerosis by in vivo magnetic resonance imaging detect lesion regression after correction of dyslipidemia. *Arterioscler. Thromb. Vasc. Biol. 24*, 1714−9.
(29) Amirbekian, V., Lipinski, M. J., Briley-Saebo, K. C., Amirbekian, S., Aguinaldo, J. G., Weinreb, D. B., Vucic, E., Frias, J. C., Hyafil, F., Mani, V., Fisher, E. A., and Fayad, Z. A. (2007) Detecting and assessing macrophages in vivo to evaluate atherosclerosis noninvasively using molecular MRI. *Proc. Natl. Acad. Sci. U. S. A. 104*, 961−6.
(30) Cormode, D. P., Briley-Saebo, K. C., Mulder, W. J., Aguinaldo, J. G., Barazza, A., Ma, Y., Fisher, E. A., and Fayad, Z. A. (2008) An ApoA-I mimetic peptide high-density-lipoprotein-based MRI contrast agent for atherosclerotic plaque composition detection. *Small 4*, 1437−44.
(31) Sieber, M. A., Pietsch, H., Walter, J., Haider, W., Frenzel, T., and Weinmann, H. J. (2008) A preclinical study to investigate the development of nephrogenic systemic fibrosis: A possible role for gadolinium-based contrast media. *Invest. Radiol. 43*, 65−75.
(32) Barge, A., Cravotto, G., Gianolio, E., and Fedeli, F. (2006) How to determine free Gd and free ligand in solution of Gd chelates. A technical note. *Contr. Media Mol. Imaging 1*, 184−188.
(33) Kane, J., Havel, R. Chapter 114: Introduction: Structure and Metabolism of Plasma Lipoproteins, In *Scriver's Online Metabolic and Molecular Bases of Inherited Disease*, McGraw Hill, http://www.ommbid.com/.
(34) Kahlon, T. S., Glines, L. A., and Lindgren, F. T. (1986) Analytic ultracentrifugation of plasma lipoproteins. *Methods Enzymol. 129*, 26−45.
(35) Stathopulos, P. B., Scholz, G. A., Hwang, Y. M., Rumfeldt, J. A., Lepock, J. R., and Meiering, E. M. (2004) Sonication of proteins causes formation of aggregates that resemble amyloid. *Protein Sci. 13*, 3017−27.
(36) Stein, O., and Stein, Y. (2005) Lipid transfer proteins (LTP) and atherosclerosis. *Atherosclerosis 178*, 217−30.
(37) Tall, A. (1995) Plasma lipid transfer proteins. *Annu. Rev. Biochem. 64*, 235−57.
(38) Jiang, X. C. (2002) The effect of phospholipid transfer protein on lipoprotein metabolism and atherosclerosis. *Front. Biosci. 7*, d1634−41.
(39) Massey, J. B., Gotto, A. M., Jr., and Pownall, H. J. (1982) Kinetics and mechanism of the spontaneous transfer of fluorescent phosphatidylcholines between apolipoprotein-phospholipid recombinants. *Biochemistry 21*, 3630−6.
(40) Rao, R., Albers, J. J., Wolfbauer, G., and Pownall, H. J. (1997) Molecular and macromolecular specificity of human plasma phospholipid transfer protein. *Biochemistry 36*, 3645−53.
(41) Parhofer, K. G., and Barrett, P. H. (2006) Thematic review series: patient-oriented research. What we have learned about VLDL and LDL metabolism from human kinetics studies. *J. Lipid Res. 47*, 1620−30.
(42) Eder, H. A. (1957) The lipoproteins of human serum. *Am. J. Med. 23*, 269−82.
(43) Florsheim, W. H., and Morton, M. E. (1957) Stability of phospholipid binding in human serum lipoproteins. *J. Appl. Physiol. 10*, 301−4.
(44) Kunkel, H. G., and Bearn, A. G. (1954) Phospholipid studies of different serum lipoproteins employing P32. *Proc. Soc. Exp. Biol. Med. 86*, 887−91.
(45) Nordestgaard, B. G., Hjelms, E., Stender, S., and Kjeldsen, K. (1990) Different efflux pathways for high and low density lipoproteins from porcine aortic intima. *Arteriosclerosis 10*, 477−85.
(46) Nordestgaard, B. G., Tybjaerg-Hansen, A., and Lewis, B. (1992) Influx in vivo of low density, intermediate density, and very low density lipoproteins into aortic intimas of genetically hyperlipidemic rabbits. Roles of plasma concentrations, extent of aortic lesion, and lipoprotein particle size as determinants. *Arterioscler. Thromb. 12*, 6−18.
(47) Stender, S., and Hjelms, E. (1988) In vivo transfer of cholesteryl ester from high and low density plasma lipoproteins into human aortic tissue. *Arteriosclerosis 8*, 252−62.
(48) Stender, S., and Zilversmit, D. B. (1981) Transfer of plasma lipoprotein components and of plasma proteins into aortas of cholesterol-fed rabbits. Molecular size as a determinant of plasma lipoprotein influx. *Arteriosclerosis 1*, 38−49.
(49) Nordestgaard, B. G., and Zilversmit, D. B. (1988) Large lipoproteins are excluded from the arterial wall in diabetic cholesterol-fed rabbits. *J. Lipid Res. 29*, 1491−500.
(50) Feig, J. E., Rong, J. X., Shamir, R., Sanson, M., Vengrenyuk, Y., Liu, J., Rayner, K., Moore, K., Garabedian, M., and Fisher, E. A. (2011) HDL promotes rapid atherosclerosis regression in mice and alters inflammatory properties of plaque monocyte-derived cells. *Proc. Natl. Acad. Sci. U. S. A. 108*, 7166−71.
(51) Parks, J. S., Li, H., Gebre, A. K., Smith, T. L., and Maeda, N. (1995) Effect of apolipoprotein A-I deficiency on lecithin:cholesterol acyltransferase activation in mouse plasma. *J. Lipid Res. 36*, 349−55.
(52) Ishibashi, S., Goldstein, J. L., Brown, M. S., Herz, J., and Burns, D. K. (1994) Massive xanthomatosis and atherosclerosis in cholesterol-fed low density lipoprotein receptor-negative mice. *J. Clin. Invest. 93*, 1885−93.
(53) Olin-Lewis, K., Benton, J. L., Rutledge, J. C., Baskin, D. G., Wight, T. N., and Chait, A. (2002) Apolipoprotein E mediates the retention of high-density lipoproteins by mouse carotid arteries and cultured arterial smooth muscle cell extracellular matrices. *Circ. Res. 90*, 1333−9.
(54) Rutledge, J. C., Mullick, A. E., Gardner, G., and Goldberg, I. J. (2000) Direct visualization of lipid deposition and reverse lipid transport in a perfused artery: roles of VLDL and HDL. *Circ. Res. 86*, 768−73.